

UNIVERSITY OF
Waterloo



Department of Mechanical and Mechatronics Engineering

**ME362 Project 2 - Analysis, Modeling, and
Optimization of a Frisbee**

A Report Prepared For:
Professor Sean D. Peterson

Prepared By:
Evan Kwon (21013390)
Makis Lam (20994505)
Ivan Lin (21021898)
Robert List (21030790)

2nd December 2025

Table of Contents

1 Historical Development of Frisbee	1
1.1 Early History	1
1.2 History of Discs used in Ultimate Frisbee	1
1.3 Different Types of Discs	2
2 Engineering Analysis	3
2.1 Shape of a Disc	3
2.2 Disc Orientation Coordinate System	4
2.3 Forces on a Disc	4
2.3.1 Gravity	4
2.3.2 Drag Force	4
2.3.3 Lift Force	5
2.4 Effects of Spin on a Disc	6
2.5 Effects of Reynolds Number	7
2.6 Modeling Objective	7
3 Modeling	8
3.1 Free Diagram Modeling	8
3.2 2D Simplified Case	8
3.3 3D Case with Spin and Angle of Attack	10
3.4 Implementation and Assumptions in Python	13
4 Justification and Limitations of the Frisbee Model	16
4.1 Justification & Validation of Model	16
4.2 Limitations	19
5 Optimization of the Frisbee Throw	21
5.1 Implementation into Optimization Script	21
5.2 Results and Analysis	21
References	24

List of Figures

1	Wham-O's "Pluto Platter" disc	1
2	Discraft's "Ultrastar" disc	1
3	eurodisc, competitive level Ultimate disc	2
4	Airfoils of different disc golf discs [8]	2
5	Cross section of airfoil (left) and disc (right) [10]	3
6	Lift coefficient C_L versus angle of attack α [12]	6
7	Free body diagram of a disc	8
8	fssh3 Simulated Flight Trajectory	17
9	f2302 Simulated Flight Trajectory	18
10	Optimized Huck Throw	22
11	Drag Coefficient vs Angle of Attack	23

List of Tables

1	Initial conditions for Flight fssh3 used in the model validation.	16
2	Initial conditions for Flight f2302 used in the model validation.	18

1 Historical Development of Frisbee

1.1 Early History

The first development in the history of the modern-day frisbee happened in the late 1930s when American inventor Walter Frederick Morrison founded a business selling flying discs on a beach in Los Angeles. These flying discs were simply cake pans, which Morrison bought for 5¢ and sold for 25¢ at the time [1]. After serving in the Second World War, Morrison and his business partner, Warren Franscioni, started the development of an improved plastic flying disc. In 1948, they finished development of the first plastic disc which they named “Flyin-Saucer” [2]. In the early 1950s, Morrison and Franscioni ended their partnership, and Morrison started his own company in 1954 to continue selling the “Flyin-Saucer”. Morrison discovered that rather than relying on Southern California Plastics, the company that had been

molding the frisbees up to now, he could produce discs more cheaply himself. In 1955, he invented the “Pluto Platter”, which became the model for all modern discs. In 1957, Morisson sold all rights to Wham-O [1].

Later that year, executives at Wham-O renamed the “Pluto Platter” to “Frisbee”, after discovering that college students were using this name to refer to the “Pluto Platter” [2].



Figure 1: Wham-O’s “Pluto Platter” disc

1.2 History of Discs used in Ultimate Frisbee

In the late 1960s and early 1970s, when Ultimate Frisbee was becoming a more official sport with concrete rules and regulations, teams would play with the “Master” disc. This disc was developed by Wham-O based on the “Pluto Platter” and was deliberately advertised as a sporting disc rather than recreational [3].

In 1977, Wham-O released another disc, the World Class “80 Mold” disc. The “80 Mold” weighed 165 grams, and was much less flimsy than the “Master” disc. In addition to this, it was also more stable and consistent, even in windy conditions. The “80 Mold” was quickly adopted as the standard disc for play and was used widely even after it was discontinued in 1983 [4].



In 1981 Discraft, a company founded in London, Ontario in the 1970’s introduced a competing disc, aiming to replace the “80 Mold”. Named the “Ultrastar”, the Discraft disc weighed in at 175 grams. After an update to the mold in 1983, it began to increase

Figure 2: Discraft’s “Ultrastar” disc

in popularity. In the mid to late 1980's the "Ultrastar" was adopted for ultimate. Wham-O introduced a competing disc, the "U-Max", also weighing 175 grams. However, due to quality issues it was never widely accepted [5]. In 1991 the "Ultrastar" became the standard disc in UPA tournament play. To this day it remains the standard disc [6].

Today there are many different regulation discs, which are all still based on the "Pluto Platter" design. Different Ultimate regions use different discs. For example, while the "Ultrastar" is still the most widely used disc, some European leagues use the "eurodisc" 4.0 Organic. Discs regulations discs have a diameter of 27.3 cm and weigh 175 grams to ensure consistency between games [7].



*Figure 3: eurodisc, competitive level
Ultimate disc*

1.3 Different Types of Discs

Although the disc used in Ultimate Frisbee has remained relatively unchanged since the "Pluto Platter", other sports and activities have very differently designed discs. Perhaps the best example is the discs used in disc golf. Disc golf discs are smaller than Ultimate discs, having a minimum diameter of 21 cm. The shape of the disc also varies widely per disc [8]. Each disc is optimized for a certain distance or path. In general, there are three main shapes: driver, mid-range, and putter, shown in Figure 4. The driver has a sharp airfoil to allow for fast, long throws, at the price of stability. The putter has a much more blunt airfoil, making it best for short-range, stable, accurate throws [8]. There are hundreds of different airfoil shapes to choose from, akin to choosing a club in golf.

Standard Classes of Golf Discs		
	Driver	The sharper edge makes a driver built for speed.
	Midrange	Less distance than a driver, but more control.
	Putter	For slow and highly controlled flights to the basket.

Figure 4: Airfoils of different disc golf discs [8]

Other unique discs have been developed, optimized to different objectives. For example, the Aerobie flying ring is a ring-shaped flying disc designed to be thrown long distances at high speed. The Aerobie ring is only 3 mm in thickness, which gives it very little drag, allowing it to fly far distances [9]. Other discs have been optimized for recreational use, such as discs that float in water, or discs which are more stable and slow, allowing for easy throwing and catching.

2 Engineering Analysis

2.1 Shape of a Disc

The shape of a disc can be described as a circular plate body, having a domed surface along the edge that flattens out moving towards the centre. The underside is comparatively flat, while featuring a thick, rounded rim along the perimeter. Looking at this geometry's cross-section in Figure 5, it resembles a cambered airfoil.

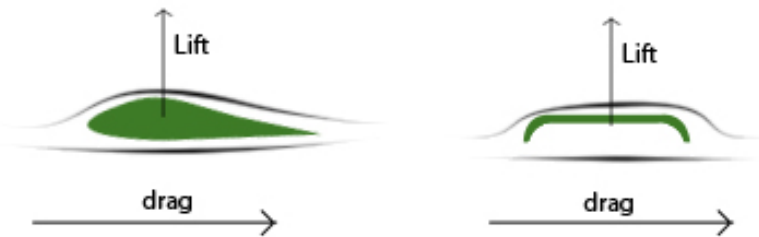


Figure 5: Cross section of airfoil (left) and disc (right) [10]

This cross-section is intentional as it mimics an airfoil's curved upper surface and flatter underside to create a pressure gradient that accelerates airflow and generates lift. As the flow travels over the upper surface, the curvature forces the streamlines to bend. Particles moving in a curved path must accelerate toward the centre of curvature, which requires a centripetal acceleration. This can be provided by a pressure difference across the streamline.

When omitting gravity and only looking at horizontal flow, Euler's equation in the normal direction expresses the relationship between the pressure gradient and curvature of the streamlines:

$$\begin{aligned} \frac{1}{\rho} \frac{\partial P}{\partial n} + g \frac{\partial z}{\partial n} &= \frac{V^2}{R} \\ \Rightarrow \frac{1}{\rho} \frac{\partial P}{\partial n} &= \frac{V^2}{R} \end{aligned}$$

This equation shows that pressure increases outward from the centre of curvature. As a result, the pressure closest to the airfoil's top surface is lower than the pressure away from the surface. The resulting pressure gradient produces a net force directed toward the center of curvature, providing the centripetal acceleration required to bend the streamlines. On the underside of the airfoil, if the surface is flat or even slightly curved,

the pressure remains higher than on the upper surface due to the upper surface's stronger curvature. This combined effect creates a net upward force (lift).

2.2 Disc Orientation Coordinate System

The orientation of a disc in 3D space can be described by yaw, pitch, and roll: yaw is the rotation about the vertical axis, pitch is the rotation about the sideways axis, and roll is the rotation about the forward axis.

2.3 Forces on a Disc

Several forces act on a disc in flight. These are: gravity, drag force, and lift force. While gravity remains constant throughout the disc's flight, the lift and drag forces are continually changing due to changes in the magnitude and direction of the wind velocity vector, the orientation of the disc in relation to that wind vector, the disc's spin rate, etc. These forces are elaborated on below.

2.3.1 Gravity

Gravity is a constant downward force that acts on the centre of mass of the disc. Unlike the aerodynamic forces (lift and drag), gravity is not dependent on external parameters such as angle of attack or wind velocity; it is dependent only on the mass of the disc.

2.3.2 Drag Force

Drag force always acts opposite and parallel to the disc's velocity vector. The magnitude of the drag force F_D is represented by:

$$F_D = \frac{1}{2} C_D \rho V^2 A \quad (1)$$

Where C_D is the drag coefficient of the body, ρ is the density of the fluid being traveled through, V is the velocity of the body relative to the fluid, and A is the frontal area (the area "seen" by the flow) of the object.

There are two parts to the drag coefficient. Form drag, C_{D0} , which is the drag at zero lift, and induced drag, $C_{D\alpha}$, which affects finite, lifting bodies, such as a disc. For a disc, C_D can be expressed by the following function from Hummel's 2003 thesis [11]:

$$C_D = C_{D0} + C_{D\alpha}(\alpha - \alpha_0)^2 \quad (2)$$

Where α is the angle of attack of the disc, and α_0 is the angle of attack that produces zero lift. for most frisbees, $\alpha_0 = -4^\circ$ [11]. To define the angle of attack, the chord line must be defined first. It is a straight line that connects the leading and trailing edges of an airfoil; the angle of attack is then the angle the chord

line forms with the relative wind velocity vector. It can be seen in Equation 2 that C_D is a quadratic function of the angle of attack. As α increases, so too does the drag experienced by the disc.

2.3.3 Lift Force

Lift is defined as the component of force perpendicular to the direction of motion. In the context of throwing a frisbee, the lift force generally opposes the force of gravity since the direction of motion is roughly horizontal. Lift on a frisbee is generated by the shape of the disc. As mentioned in Section 2.1, the cross-sectional geometry of a disc creates a pressure differential at the upper surface, accelerating airflow at the top of the disc. As the bottom of the disc has a weaker curvature, the pressure there will always be greater than the top surface. The resulting difference in pressure generates lift. The equation for lift force can be derived from Bernoulli's equation for fluid flow:

$$\frac{v_1^2}{2} + \frac{p_1}{\rho} + gh_1 = \frac{v_2^2}{2} + \frac{p_2}{\rho} + gh_2 \quad (3)$$

Assuming the height difference is negligible ($h_1 - h_2 \approx 0$) and defining the velocity relationship $v_1 = Cv_2$:

$$\frac{C^2 v_2^2}{2} + \frac{p_1 - p_2}{\rho} - \frac{v_2^2}{2} = 0 \quad (4)$$

Substituting the definition of lift pressure:

$$\begin{aligned} \frac{F_L}{A} &= p_1 - p_2 \\ \Rightarrow \frac{C^2 v_2^2}{2} + \frac{F_L}{\rho A} - \frac{v_2^2}{2} &= 0 \end{aligned}$$

Rearranging for the Lift Force F_L :

$$\begin{aligned} \frac{v_2^2(C^2 - 1)}{2} &= -\frac{F_L}{\rho A} \\ F_L &= \frac{1}{2} \rho A v_2^2 (1 - C^2) \end{aligned}$$

By letting the lift coefficient $C_L = 1 - C^2$, the standard lift equation form is derived.

$$F_L = \frac{1}{2} C_L \rho V^2 A_p \quad (5)$$

Where C_L is the lift coefficient of the body, ρ is the density of the fluid being traveled through, V is the velocity of the body relative to the fluid, and A_p is the planform area (the area projected from above) of the object.

Like the drag coefficient, the lift coefficient is a function of angle of attack. The relationship between the two parameters follows a curve, as shown below:

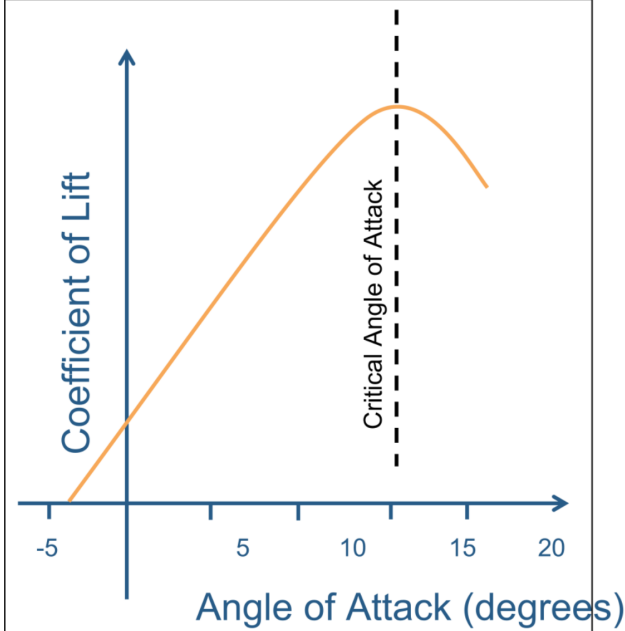


Figure 6: Lift coefficient C_L versus angle of attack α [12]

It can be seen that C_L increases with α until some critical angle of attack, α_{cr} , at which point stall occurs. If α continues to increase beyond α_{cr} , the lift force experienced by the body begins to decrease. For small angles of attack (like those seen when throwing a frisbee), C_L follows a linear relationship with α , and can be approximated using the following relationship [11]:

$$C_L = C_{L0} + C_{L\alpha}\alpha \quad (6)$$

Where C_{L0} is the lift coefficient at $\alpha = 0$ and $C_{L\alpha}$ is the slope of the linear region.

Both drag and lift forces do not act on the centre of mass (COM) of the disc, instead they act on the disc's centre of pressure (COP). Since the COP lies some distance away from the COM, both drag and lift forces impart moments on the frisbee, causing it to pitch up or down. These aerodynamic moments are elaborated upon in Section 3.2.

2.4 Effects of Spin on a Disc

The amount of spin imparted on a disc when thrown affects the stability of the disc during flight by increasing the disc's angular momentum. Much like how objects with high linear momentum are more resistant to

changes in direction from small forces, objects with high angular momentum are more resistant to changes in the direction of their rotating axis by small torques. Angular momentum of a body is calculated by the following formula:

$$L = I\omega \quad (7)$$

Where L is angular momentum, I is the object's moment of inertia, and ω is the angular velocity (spin rate) of the object. By increasing ω , the angular momentum vector (collinear with the disc's axis of rotation) becomes large and makes the disc more resilient to changes in orientation due to aerodynamic torques.

2.5 Effects of Reynolds Number

The Reynolds number compares the inertial forces to the viscous forces in a flow. For a disc, it depends on the air density ρ , disc speed v , disc diameter D , and air viscosity μ . The equation is expressed as:

$$Re = \frac{\rho v D}{\mu} \quad (8)$$

Reynolds number has a significant influence to how air flows around the disc. During the disc release stage of a frisbee throw, where disc speed is high, the Reynolds number is at its maximum, resulting in a predominantly turbulent boundary layer. Turbulent boundary layers carry more momentum close to the surface, allowing the boundary layer to stay attached to the upper surface for longer distances. This delay in flow separation helps reduce pressure drag. In contrast, the Reynolds number becomes lower as the disc slows down, and the boundary layer loses momentum much easier, making the flow more likely to separate. At this point, the pressure difference weakens, and the pressure drag dominates, causing the disc to slow down and drop.

In real-world situations, Reynolds number affects aerodynamic coefficients such as lift C_L and drag C_D , in addition to angle of attack. This makes C_L and C_D a function of angle of attack α and Re_D , $f(\alpha, Re_D)$.

2.6 Modeling Objective

The objective of this report is to build and analyze a model that determines the optimal throwing parameters for a frisbee that result in the furthest travel, given an initial velocity. The modeling will be broken into two parts. The first will be a simplified 2D model that neglects spin rate and angle of attack. The second will analyze a more complex and realistic 3D case that takes spin rate and angle of attack into consideration.

3 Modeling

3.1 Free Diagram Modeling

The modeling started by decomposing the disc's instantaneous velocity \vec{V} into its vertical and horizontal components (V_x, V_y). Then the drag force F_D was defined opposing the direction of motion of the disc, and the lift force F_L perpendicular to the direction of motion. Weight F_g was defined to act downward. The disc was then drawn at an angle of attack α , relative to the x -axis. This is illustrated in Figure 7.

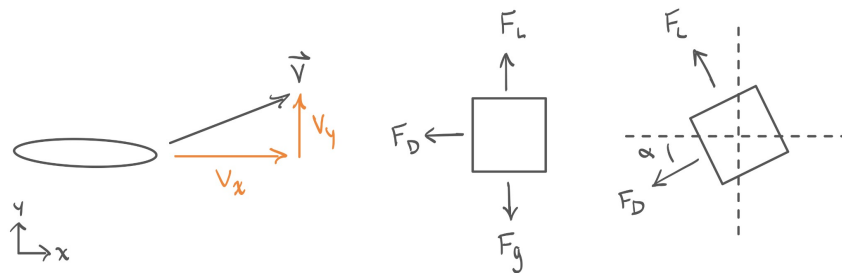


Figure 7: Free body diagram of a disc

3.2 2D Simplified Case

To model and predict the aerodynamic forces on the disc, key assumptions must be made to simplify the model. The first case will be simplified into a 2D model without the effects of spin (gyroscopic effects) or angle of attack. This will then be iterated on to add in these additional factors and add complexity to the model.

Assumptions:

- Frisbee is a cambered airfoil but treated as a point mass
- Quasi-steady Aerodynamics (C_D & C_L are steady)
- Fluid is Newtonian ($\mu = \text{constant}$)
- Fluid is Incompressible ($\rho = \text{constant}$)
- No Spin ($\omega = 0$)
- No Angle of Attack ($\alpha = 0$)
- Environment is at SATP ($P = 1\text{atm}$, $T = 298.15K$)
- No Wind
- Initial conditions of V

- Constant Acceleration due to Gravity ($g = 9.81 \text{ m/s}^2$)

The properties of the disc must also be defined to base everything around the same geometry. The mass and diameter of the disc are defined based on the Ultrastar 175 g frisbee [11].

$$\left. \begin{array}{l} D = 0.26 \text{ m} \\ m = 0.175 \text{ kg} \end{array} \right\}$$

Reynolds Number Calculation

The Reynolds number (Re) is calculated using the characteristic diameter of the frisbee ($D = 0.26 \text{ m}$) and standard air properties. The velocity of $v = 14 \text{ m/s}$ is used as it is the average speed of a frisbee throw.

$$Re = \frac{\rho v D}{\mu} = \frac{(1.184 \text{ kg/m}^3)(14 \text{ m/s})(0.26 \text{ m})}{18.37 \times 10^{-6} \text{ Ns/m}^2}$$

$$Re \approx 234608.6$$

Lift & Drag Force Model

Knowing the Reynolds Number and the previously derived lift and drag equations, these can be used along with the empirical drag and lift coefficients found in the model. Some sample values are like $C_{D0} = 0.18$, $C_{D\alpha} = 0.69$, $C_{L0} = 0.33$, and $C_{L\alpha} = 1.91$ [11]. These values are for short flights while Potts uses different coefficients such as $C_{D0} = 0.08$, $C_{D\alpha} = 2.72$, $C_{L0} = 0.20$, and $C_{L\alpha} = 2.96$ which were measured in a wind tunnel and are supposed to model long flights [13].

Horizontal Motion (x -direction)

Applying Newton's Second Law in the horizontal direction:

$$\sum F_x = m\ddot{x}$$

The forces acting in the x -direction are the horizontal components of Drag (F_D) and Lift (F_L):

$$m\ddot{x} = -F_D \cos \theta - F_L \sin \theta$$

Substituting the definitions of aerodynamic forces $F_D = \frac{1}{2}\rho A C_{D0} v^2$ and $F_L = \frac{1}{2}\rho A C_{L0} v^2$:

$$m\ddot{x} = -\left(\frac{1}{2}\rho A C_{D0} v^2\right) \cos \theta - \left(\frac{1}{2}\rho A C_{L0} v^2\right) \sin \theta$$

Factor out the common terms and divide by mass m :

$$\ddot{x} = -\frac{\rho Av}{2m}(C_{D0}v \cos \theta + C_{L0}v \sin \theta)$$

Vertical Motion (y -direction)

Applying Newton's Second Law in the vertical direction:

$$\sum F_y = m\ddot{y}$$

The forces acting in the y -direction are Gravity (mg) and the vertical components of Lift and Drag:

$$m\ddot{y} = -mg + F_L \cos \theta - F_D \sin \theta$$

Substituting the force definitions again:

$$m\ddot{y} = -mg + \left(\frac{1}{2}\rho A C_{L0} v^2\right) \cos \theta - \left(\frac{1}{2}\rho A C_{D0} v^2\right) \sin \theta$$

Dividing by mass m and grouping terms:

$$\ddot{y} = -g + \frac{\rho Av}{2m}(C_{L0}v \cos \theta - C_{D0}v \sin \theta)$$

This provides two equations of motion that govern the frisbee's flight: one for the vertical motion and one for the horizontal motion. This model, however, is not very realistic as the gyroscopic effects provide stability for flight, but overall, it provides a good basis for understanding the more complex model.

3.3 3D Case with Spin and Angle of Attack

Looking at the more complicated version, a new set of assumptions must be used.

Assumptions:

- Frisbee is a cambered airfoil and treated as a rigid body
- Quasi-steady Aerodynamics (C_D & C_L are steady)
- Fluid is Newtonian ($\mu = constant$)
- Fluid is Incompressible ($\rho = constant$)
- Spin is non-zero ($\omega \neq 0$), constant, and independent of lift and drag coefficients
- Angle of Attack is not negligible ($\alpha \neq 0$), constant, and C_L and C_M are linear functions of α
- Environment is at SATP ($P = 1atm$, $T = 298.15K$)
- No Wind

- Initial conditions of V
- Constant Acceleration due to Gravity ($g = 9.81 \text{ m/s}^2$)

The flight dynamics of the frisbee are modeled using the Newton-Euler formulation for a rigid body with six degrees of freedom. The motion is described in a body-fixed coordinate frame attached to the disc, where the x-axis points forward, the y-axis points to the right, and the z-axis points downward.

Aerodynamic Moments

The aerodynamic moments acting on the disc are parameterized using linearized coefficients. Based on the experimental data from Hummel (2003) [11], the Roll (L), Pitch (M), and Yaw (N) moments are defined as:

$$\begin{aligned} L_{aero} &= (C_{R_r}r + C_{R_p}p) \frac{1}{2}\rho v^2 Ad \\ M_{aero} &= (C_{M_0} + C_{M_\alpha}\alpha + C_{M_q}q) \frac{1}{2}\rho v^2 Ad \\ N_{aero} &= (C_{N_r}r) \frac{1}{2}\rho v^2 Ad \end{aligned}$$

Where:

- p, q, r are the roll, pitch, and yaw angular rates.
- d is the diameter of the disc.
- C_{M_α} captures the dependence of pitching moment on the angle of attack α .

These equations are solved to understand the instantaneous external torques being applied to the frisbee by the fluid at any given time, which are then coupled to the following differential equations that model the kinematics of the frisbee.

Translational Motion

Applying Newton's Second Law in the rotating body frame, the sum of external forces \vec{F} relates to the linear acceleration $\dot{\vec{v}}$ and the Coriolis/centrifugal terms induced by the frame rotation $\vec{\omega} \times \vec{v}$:

$$\vec{F} = m(\dot{\vec{v}} + \vec{\omega} \times \vec{v})$$

Expanding this vector equation into scalar components for Surge (u), Sway (v), and Heave (w):

$$\begin{bmatrix} F_x \\ F_y \\ F_z \end{bmatrix} = m \left(\frac{d}{dt} \begin{bmatrix} u \\ v \\ w \end{bmatrix} + \begin{bmatrix} p \\ q \\ r \end{bmatrix} \times \begin{bmatrix} u \\ v \\ w \end{bmatrix} \right)$$

This yields the three coupled differential equations for translation:

$$F_x = m(\dot{u} + qw - rv) \quad (\text{Surge})$$

$$F_y = m(\dot{v} + ru - pw) \quad (\text{Sway})$$

$$F_z = m(\dot{w} + pv - qu) \quad (\text{Heave})$$

The term ru in the sway equation represents the Magnus-like effect where spin (r) and forward speed (u) induce a lateral force.

Rotational Motion (Euler's Equations)

The rotational dynamics are governed by Euler's equations of motion. For a body with a diagonal inertia tensor \mathbf{I} , the sum of external moments \vec{M} is:

$$\vec{M} = \mathbf{I}\dot{\vec{\omega}} + \vec{\omega} \times (\mathbf{I}\vec{\omega})$$

Given the radial symmetry of the frisbee, the moments of inertia about the diameter axes are equal ($I_{xx} = I_{yy} = I_d$), and the axial moment of inertia is $I_{zz} = I_a$. Substituting these into the cross-product yields the scalar equations:

$$L_{roll} = I_d\dot{p} + (I_a - I_d)qr$$

$$M_{pitch} = I_d\dot{q} + (I_d - I_a)pr$$

$$N_{yaw} = I_a\dot{r}$$

Gyroscopic Precession

The term $(I_d - I_a)pr$ in the pitch equation demonstrates the gyroscopic coupling. If a pitching moment M_{pitch} is applied (due to aerodynamic lift offset), it does not simply cause a pitch acceleration \dot{q} . Instead, because the spin rate r is large, the equation balances by inducing a roll rate p . This mathematical derivation explains why a frisbee rolls (banks) to the side rather than flipping end-over-end.

3.4 Implementation and Assumptions in Python

Understanding the derivations from above yields 12 governing equations for the 6 DOF frisbee model. There are 3 DEs for translational motion and 3 that govern rotational motion, 3 that relate the frisbee's angular rates to the rate of change of the Euler Angles (describing the orientation relative to the earth), and the 3 DEs that transform the frisbee-frame velocity into Earth-frame coordinates. The other 6 equations not listed above are:

$$\begin{bmatrix} \dot{\phi} \\ \dot{\theta} \\ \dot{\psi} \end{bmatrix} = \begin{bmatrix} 1 & \sin \phi \tan \theta & \cos \phi \tan \theta \\ 0 & \cos \phi & -\sin \phi \\ 0 & \sin \phi \sec \theta & \cos \phi \sec \theta \end{bmatrix} \begin{bmatrix} p \\ q \\ r \end{bmatrix}$$

$$\begin{bmatrix} \dot{x} \\ \dot{y} \\ \dot{z} \end{bmatrix} = [R_{body \rightarrow earth}] \begin{bmatrix} u \\ v \\ w \end{bmatrix}$$

This rotation matrix is as such where ψ is the yaw Euler angle, θ is the pitch Euler angle, and ϕ is the roll angle:

$$[R_{body \rightarrow earth}] = \begin{bmatrix} c\theta c\psi & s\phi s\theta c\psi - c\phi s\psi & c\phi s\theta c\psi + s\phi s\psi \\ c\theta s\psi & s\phi s\theta s\psi + c\phi c\psi & c\phi s\theta s\psi - s\phi c\psi \\ -s\theta & s\phi c\theta & c\phi c\theta \end{bmatrix}$$

and also 3 equations that govern the aerodynamic forces acting on the disc. These equations are complex as they contain nonlinearities and must be solved using numerical methods.

In Python there is a library called SciPy, which solves initial value problems using the Runge-Kutta 4(5) method. This method is an explicit solver where the slope at the beginning of the time step k_1 , the midpoint of the time step k_2 using k_1 , another slope at the midpoint of the time step k_3 calculated using k_2 , and the slope at the end of the time step k_4 using k_3 are calculated. After these slopes are calculated, the final update formula to the next step is calculated by:

$$y_{n+1} = y_n + \frac{h}{6}(k_1 + 2k_2 + 2k_3 + k_4)$$

A note must be made about the lift and drag coefficients being used. For this model, as there are multiple measured C_L and C_D values for different flights, the model uses a hybrid approach where it uses one set of coefficients for long flights versus short flights. This will be determined by the initial velocity, so that the coefficients used in this model are:

$$\left\{ \begin{array}{l} \text{Short Flight} \\ V < 16 \text{ m/s} \end{array} \right. \quad \left\{ \begin{array}{l} C_{L0} = 0.188 \\ C_{L\alpha} = 2.37 \\ C_{D0} = 0.15 \\ C_{D\alpha} = 1.24 \end{array} \right.$$

$$\left. \begin{array}{l} \text{Long Flight} \\ V > 16 \text{ m/s} \end{array} \right. \quad \left\{ \begin{array}{l} C_{L0} = 0.20 \\ C_{L\alpha} = 2.96 \\ C_{D0} = 0.08 \\ C_{D\alpha} = 2.60 \end{array} \right.$$

It can be seen here that the coefficients are drastically different for short vs long flights. The long flight includes greater coefficient of lift and lower drag coefficients. This helps the disc fly further, and this is likely due to the difference in boundary layer behavior, with higher velocity, that leads to a higher Reynolds Number and more turbulent flow. With more turbulent flow, that means there is more skin friction drag but lower pressure drag due to separation being delayed. Overall, this helps the disc produce more lift and less drag at higher velocities.

The problem with simply solving all of the equations is that the frisbee is a spinning object, and that means the frame of the body is also spinning. This provides a great challenge for applying the rotation matrix with standard Euler rates, as the Roll (ϕ) and Pitch (θ) angles would oscillate wildly as the "x-axis" spun around with the disc. The solution here is to "de-spin" the frame and track the orientation of the disc plane and not the specific spots on the frisbee. Thus, the spin rate r is ignored for the Pitch and Roll update.

Another issue that needed to be overcome while implementing the logic into the Python solver was related to the fact that Newton's Second Law only works within an inertial frame. For the rotating disc, there are fictitious forces like centrifugal or Coriolis that must be added to make $F = ma$ work. However if the accelerations are solved for using the body frame, there are forces that are no longer valid. This leads to unexpected behaviors such as death spiral. So the solution taken to implement the logic is that the forces are calculated in the body frame, then transformed into the earth frame to then calculate the translational accelerations.

4 Justification and Limitations of the Frisbee Model

4.1 Justification & Validation of Model

To validate the model, empirical data is required to ensure that similar inputs lead to similar results and that the model will accurately predict the real-life behavior of the disc. The empirical data were taken from the flight data of Hummel in an earlier thesis. These are the input parameters used displayed in Table 1 [14]:

Table 1: Initial conditions for Flight fssh3 used in the model validation.

Parameter	Input Data (fssh3)
Velocity (V_0)	3.77 m/s
Spin Rate (r)	85.0
Release Height	1.13 m
Angle of Attack (α)	35.90°
Roll/Tilt (ϕ)	-3.80°
Release Angle (ψ)	-8.45°
Launch Angle (γ)	-16.40°

With these values, the simulation can use them as initial input variables and calculate the overall trajectory of the flight. These are the results as shown in Figure 9:

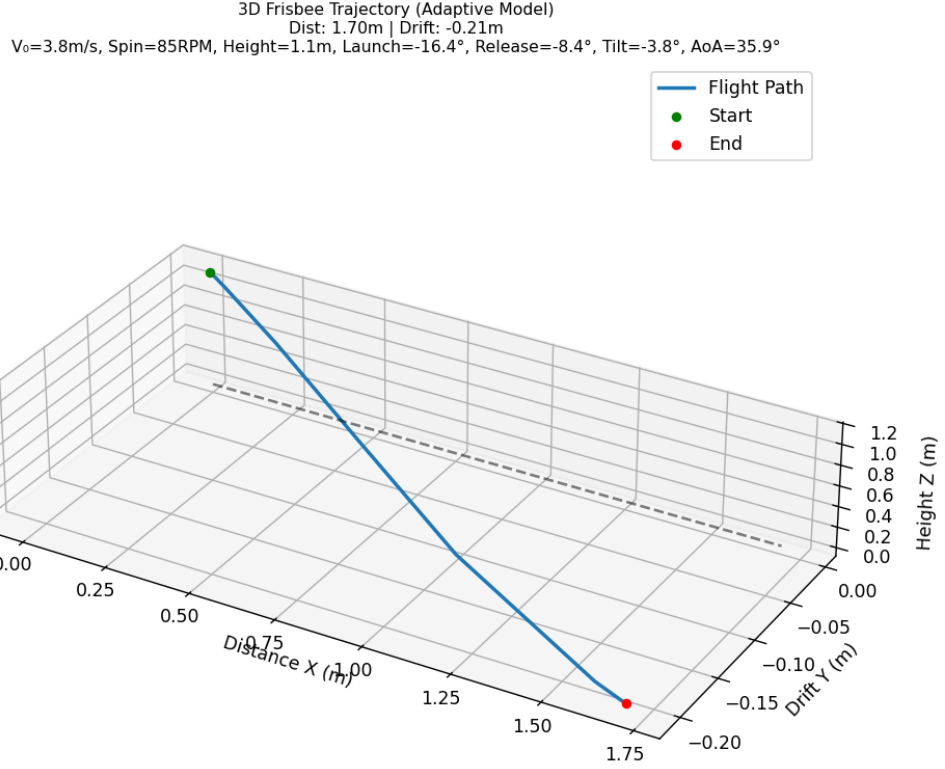


Figure 8: fssh3 Simulated Flight Trajectory

This shows that the simulation very closely matches the flight data as the distance covered in x direction for the simulation is $x = 1.70 \text{ m}$ vs the flight data where distance covered was $x = 1.62 \text{ m}$. The distance in y was also very similar with $y = -0.21 \text{ m}$ vs $y = 0.1 \text{ m}$ for simulation vs flight data, respectively [14].

To validate, using one more case, flight f2302 will be used for comparison. This data is taken from the Hummel 2003 paper as shown in Table 2.

Table 2: Initial conditions for Flight f2302 used in the model validation.

Parameter	Input Data (fssh3)
Velocity (V_0)	13.42 m/s
Spin Rate (r)	518.0
Release Height	1.2 m
Angle of Attack (α)	1.7°
Roll/Tilt (ϕ)	-4.0°
Release Angle (ψ)	-1.8°
Launch Angle (γ)	0.0°

Using these initial conditions the simulation is ran, and the results are as follows:

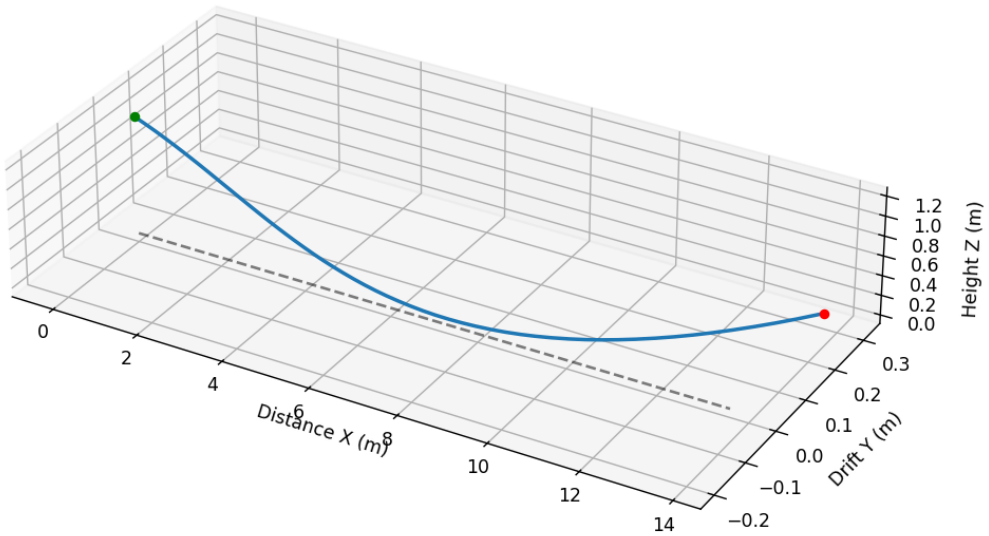
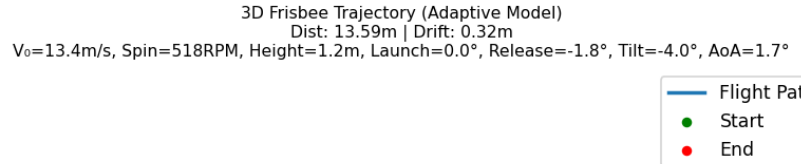


Figure 9: f2302 Simulated Flight Trajectory

This simulation shows a close correlation with the experimental results, with a distance traveled of $x = 13.59\text{ m}$ versus $x = 15\text{ m}$ in the experimental data. This difference in distance represents a 9.4% error,

which for a basic model is acceptable. Using these empirical flight test data and matching them to the simulated results, the model is validated.

4.2 Limitations

Firstly, this model oversimplifies the aerodynamic coefficients. The model assumes quasi-steady aerodynamics, meaning coefficients of lift and drag respond instantaneously to velocity and angle of attack. In the model, these coefficients only depend on the angle of attack, unlike in real-world flight where they are also affected by the Reynolds number. The change of disc speed would influence Re_D , and thus, C_L and C_D . Without incorporating the effects of Reynolds number, the model cannot accurately model late-stage flight or boundary layer behaviors.

Additionally, because the angle of attack α is treated as constant and calculated at each time step, C_D and C_L are linear functions of α . This limits the model's ability to simulate dynamic responses, and non-linear stall characteristics are not fully captured. A better approach is to include the local induced angle of attack to see which parts of the disc have different coefficients of lift and drag, and account for local stalls. Further, the spin rate is also treated as constant with no decay, when in reality, it should gradually slow down due to air friction and gyroscopic damping.

Although the model treats angle of attack and spin rate as constant, this assumption can be partially justified for high-spin throws. A high spin rate allows the disc to maintain its angle of attack due to high angular momentum and thus gyroscopic stability. While this does not eliminate the inaccuracy of holding the angle of attack constant, it can be a reasonable approximation for high-spin flights.

In the model, spin and velocity are inputted as independent variables; however, this does not accurately model human abilities, as these two parameters are coupled by the amount of energy that a player can exert in a throw. The independence enables the simulation to have unrealistic combinations, but this is not a huge concern, as it can be solved by choosing realistic combinations.

Lastly, this model does not incorporate disturbances during flight, such as wind. Frisbee flight is heavily influenced by crosswinds and turbulence, which can create extra lift or cause the disc to prematurely drop.

In conclusion, the simulation is most accurate for short-duration, high-speed, high-spin flights, where changes in Reynolds number, spin decay, and angle-of-attack variation are minimal. It can also be reliable in capturing the effects of different throwing parameters (velocity, spin, tilt, release angle) in the early

flight stages. As a result, the model can accurately predict early-flight behavior and the general trajectory shape for strong, well-thrown discs.

5 Optimization of the Frisbee Throw

5.1 Implementation into Optimization Script

Now that the model is created, implemented in Python, and validated, the best way to throw the frisbee can be found. This will be done using an optimization script that runs the model under using various initial conditions under reasonable bounds for professional frisbee players. The throw that will be optimized is the long frisbee huck, and it will be optimized for maximum distance in the x -direction. The drift in the y -direction will also be minimized. The variables being tweaked will be:

$$\left\{ \begin{array}{l} \text{Spin } (r) : (400, 1100) \\ \text{Launch Angle } (\gamma) : (5, 25) \\ \text{Release Angle } (\psi) : (-20, 20) \\ \text{Tilt Angle } (\phi) : (-45, 45) \\ \text{Angle of Attack } (\alpha) : (-4, 15) \end{array} \right.$$

5.2 Results and Analysis

After running the optimization script these were the results as shown in Figure 10. The run time was 559.7 seconds, and it yielded these optimal parameters:

$$\left\{ \begin{array}{l} \text{Spin : } r = 1100 \text{ rpm} \\ \text{Launch : Angle } \gamma = 5.92^\circ \\ \text{Release : Angle } \psi = 20^\circ \\ \text{Tilt : Angle } \phi = -26.24^\circ \\ \text{Angle of Attack : } \alpha = -4.0^\circ \end{array} \right.$$

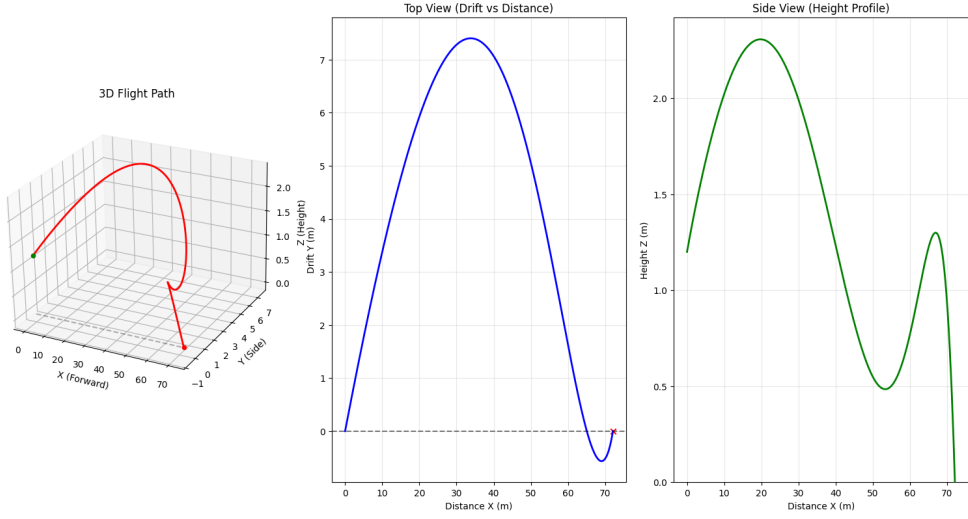


Figure 10: Optimized Huck Throw

The velocity used in this optimization was $V = 28$ m/s, as this is a typical speed for a throw of that class for professional players. It can be seen here that the best throw type is one that is called an outside-in. This throw goes towards the left, then curves back in to the right and starts with a high negative angle of tilt. This tilt angle is called a hyzer tilt, which causes the disc to drift to the left. The orientation of the disc starts with a hyzer tilt, then goes to flat, and afterward curls to an anhyzer tilt in the high-speed section. This occurs because of gyroscopic precession, where the aerodynamic pitching torque M_{aero} acts on the spinning disc to induce a roll rate ($\dot{\phi}$) to the right. In addition to having this negative tilt, there is an aim correction of 20° so that the disc goes straight and drifts as little as possible. The reason why this S-curve is optimal is that to get the most range means to allow for the x and y components of velocity to be active for as long as possible. If the disc were to simply go straight, there can still be velocity in the xy plane however the disc will be on the ground. Using the gyroscopic inertial effects to manipulate the path of the disc means that the disc can stay in the air for a longer amount of time, allowing the velocity components to act.

The likely reason that the angle of attack is at $\alpha = -4.0^\circ$ is that this is where the least amount of drag occurs according to the empirical experiments as shown in Figure 11 [11] [13]. With less drag, there is less resistance to motion within the x direction.

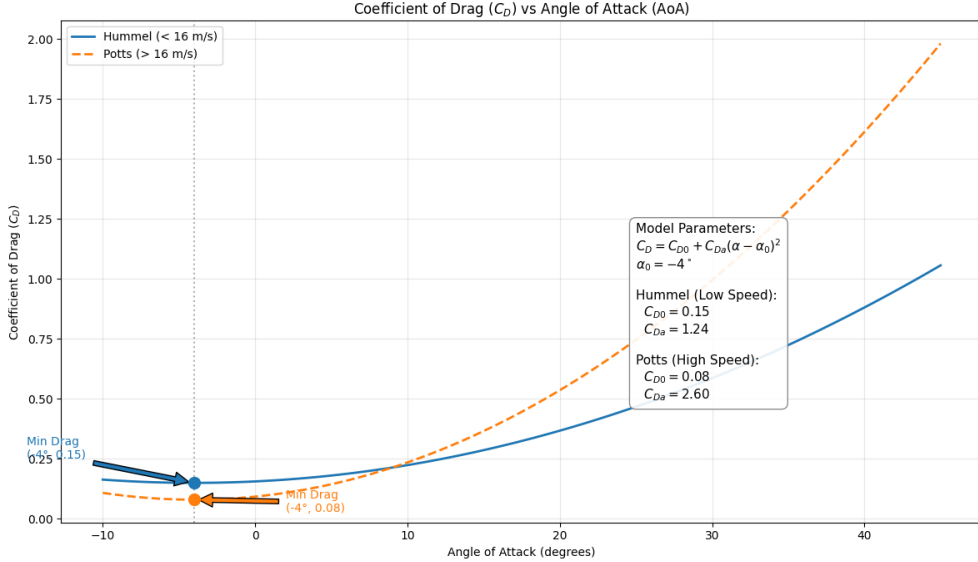


Figure 11: Drag Coefficient vs Angle of Attack

Although the optimized value shows as a negative angle of attack, there is still lift being generated that would keep the disc in the air. At $V = 28$ m/s, there is still a large amount of lift being generated to counteract the force of gravity, and this can be seen through the

Lastly, to discuss the angular velocity of the disc chosen as the optimized value, $r = 1100$ rpm, the effect of spin on the disc needs to be understood. Section 2.4 discusses some of the effects of spin on a disc, but it is interesting that out of the range of values optimized in, the highest spin value still wins. One of the reasons why the highest spin value was chosen was that the model does not fix the amount of energy from the thrower, but instead the velocity that is given to the disc, and includes the spin as a variable. It requires more energy from the thrower to get more spin on the disc, but a throw with $V = 28$ m/s with $r = 500$ rpm and $r = 1100$ rpm are very different in terms of energy required.

To expand on 2.4, spin does indeed produce more gyroscopic stability, but it is the very reason why gyroscopic precession effects occur. With more spin, more gyroscopic precession occurs, and the disc is able to curve like in the optimal S shape. It can also maintain its attitude better, keeping the same angle of attack. There are multiple reasons why having a higher spin is better, in addition to the resistance to torque. It is indeed better to have a higher spin if energy use is not a factor.

References

- [1] P. Kennedy. "The history of the frisbee®." Accessed: 2025-12-02. [Online]. Available: <https://www.flatflip.com/downloads/A%20Short%20History%20of%20the%20Frisbee.pdf>.
- [2] "'frisbee' marks 50th anniversary of name change," CTV News, Accessed: Nov. 1, 2007. [Online]. Available: http://www.ctv.ca/servlet/ArticleNews/story/CTVNews/20070616/frisbee_070616/20070616?hub=TopStories.
- [3] L. Johan. "Timeline of early history of flying disc play (1871-1995)," World Flying Disc Federation (WFDF), Accessed: Jun. 20, 2012. [Online]. Available: <http://www.wfdf.org/history-stats/history-of-flying-disc/6-timeline-of-early-history-of-flying-disc-play-1871-1995>.
- [4] "Special merit: The "80 mold'." Accessed: 2025-12-02, USA Ultimate. [Online]. Available: https://archive.usaultimate.org/about/history/hall_of_fame/80_mold_class_of_2004.aspx.
- [5] C. Eisenhood. "When wham-o was king: Why the innova v. discraft debate is old news." Accessed: 2025-12-02, Ultiworld. [Online]. Available: <https://ultiworld.com/2013/03/18/when-wham-o-was-king-why-the-innova-v-discraft-debate-is-old-news/>.
- [6] "Jim kenner and the "discraft ultra-star'." Accessed: 2025-12-02, USA Ultimate. [Online]. Available: https://archive.usaultimate.org/about/history/hall_of_fame/the_discraft_ultrastar_class_of_2011.aspx.
- [7] "Disc standards & approval," USA Ultimate, Accessed: Dec. 2, 2025. [Online]. Available: <https://usaultimate.org/programs/disc-standards/>.
- [8] "Golf discs 101 – how they are made and which ones are best," Dude Clothing, Accessed: Dec. 2, 2025. [Online]. Available: <https://www.dudeclothing.com/golf-discs-101-how-they-are-made-and-which-ones-are-best/>.
- [9] J. Cassidy, *The Aerobie Book: An Investigation Into the Ultimate Flying Mini-Machine*. Klutz Press, 1985, ISBN: 0-932592-30-9.
- [10] M. Keith. "Airfoil." Accessed: 2025-11-27. [Online]. Available: http://ffdenn2.phys.uaf.edu/211_fall2013.web.dir/Matthew_Keith/Airfoil.html.
- [11] S. A. Hummel, "Frisbee flight simulation and throw biomechanics," Ph.D. dissertation, University of California, Davis, 2003.
- [12] SKYbrary Aviation Safety. "Angle of attack (aoa)." Accessed: 2025-12-02. [Online]. Available: <https://skybrary.aero/articles/angle-attack-aoa>.

- [13] N. M. Kamaruddin, J. R. Potts, and W. J. Crowther, “Aerodynamic performance of flying discs,” *Aircraft Engineering and Aerospace Technology*, vol. 90, no. 2, pp. 347–357, 2018. DOI: 10.1108/AEAT-09-2016-0143. [Online]. Available: <https://shura.shu.ac.uk/14521/>.
- [14] M. Hubbard and S. A. Hummel, “Simulation of frisbee flight,” in *Proceedings of the 5th Conference on Mathematics and Computers in Sport*, University of Technology, Sydney, 2000.

Appendix A: 3D Model Code

```
1 # type: ignore
2 import numpy as np
3 from scipy.integrate import solve_ivp
4 import matplotlib.pyplot as plt
5 from mpl_toolkits.mplot3d import Axes3D
6 import argparse
7
8 # Try importing thermo; handle error if user hasn't installed it
9 try:
10     from thermo import Mixture # type: ignore
11     THERMO_AVAILABLE = True
12 except ImportError:
13     THERMO_AVAILABLE = False
14     print("Warning: 'thermo' library not found. Using standard air density.")
15
16 # =====
17 #   USER CONFIGURATION
18 # =====
19 AIR_TEMP_C = 25.0
20 AIR_PRESSURE_PA = 101325
21
22 # Default Throw Parameters
23 DEFAULT_V0 = 14.0
24 DEFAULT_SPIN_RPM = 600.0
25 DEFAULT_RELEASE_HEIGHT = 1.0
26
27 # Default Angles
28 DEFAULT_LAUNCH_ANGLE = 8.0
29 DEFAULT_RELEASE_ANGLE = 0.0
30 DEFAULT_TILT_ANGLE = -12.0
31 DEFAULT_ANGLE_OF_ATTACK = 4.0
32
33 # =====
34 #   OPTIMIZED DENSITY CALCULATION
35 # =====
36 # We calculate this ONCE globally to prevent slow lookups inside the loop
37 def get_global_air_density(temp_c, pressure_pa):
38     if THERMO_AVAILABLE:
39         try:
40             temp_k = temp_c + 273.15
41             air = Mixture('air', T=temp_k, P=pressure_pa)
42             return float(air.rho)
43         except:
44             return 1.225 # Fallback
45     return 1.225 # Standard sea level
46
47 # CACHED DENSITY VALUE
48 GLOBAL_rho = get_global_air_density(AIR_TEMP_C, AIR_PRESSURE_PA)
49
50 # =====
51
52 def simulate_3d_throw(v0, spin_rpm, release_height, launch_angle, release_angle,
53                       tilt_angle, aoa, temp_c, pressure_pa):
54     m = 0.175
55     g = 9.81
56
57     # Use the cached global density (Super Fast)
```

```

57     rho = GLOBAL_RHO
58
59     diameter = 0.269
60     area = 0.057
61
62     Izz = 0.00235
63     Ixx = 0.00122
64     Iyy = 0.00122
65
66     # --- DYNAMIC COEFFICIENT SELECTION (Adaptive Model) ---
67     if v0 < 16.0:
68         # HUMMEL (2003) - High Drag / Low Speed
69         CL0, CL_a = 0.188, 2.37
70         CD0, CD_a = 0.15, 1.24
71     else:
72         # POTTS & CROWTHER (2002) - Low Drag / High Speed
73         CL0, CL_a = 0.20, 2.96
74         CD0, CD_a = 0.08, 2.60
75
76     alpha_0 = -4 * np.pi/180
77
78     # Moments
79     CM0, CM_a = -0.01, -0.2
80     CR_r = -0.014
81     CN_r = -0.000034
82
83     # Initial Conditions
84     gamma = np.radians(launch_angle)
85     zeta = np.radians(release_angle)
86     vx = v0 * np.cos(gamma) * np.cos(zeta)
87     vy = v0 * np.cos(gamma) * np.sin(zeta)
88     vz = v0 * np.sin(gamma)
89
90     psi = zeta
91     alpha_rad = np.radians(aoa)
92     theta = gamma + alpha_rad
93     phi = np.radians(tilt_angle)
94
95     spin_rad_s = spin_rpm * (2 * np.pi / 60.0)
96
97     initial_state = [0, 0, release_height, vx, vy, vz, phi, theta, psi, 0, 0,
98                      spin_rad_s]
99
100    def equations(t, state):
101        x, y, z, vx, vy, vz, phi, theta, psi, wx, wy, wz = state
102
103        st, ct = np.sin(theta), np.cos(theta)
104        sp, cp = np.sin(phi), np.cos(phi)
105        ss, cs = np.sin(psi), np.cos(psi)
106        tt = np.tan(theta)
107
108        R_IB = np.array([
109            [ct*cs, ct*ss, st],
110            [sp*st*cs - cp*ss, sp*st*ss + cp*cs, -sp*ct],
111            [-cp*st*cs - sp*ss, -cp*st*ss + sp*cs, cp*ct]
112        ])
113
114        v_earth = np.array([vx, vy, vz])
115        v_body = R_IB @ v_earth

```

```

115     ub, vb, wb = v_body
116
117     vel = np.linalg.norm(v_body)
118     if vel == 0: vel = 0.001
119
120     alpha = -np.arctan2(wb, ub)
121
122     cl = CL0 + CL_a * alpha
123     cd = CD0 + CD_a * (alpha - alpha_0)**2
124     cm = CM0 + CM_a * alpha
125
126     q_dyn = 0.5 * rho * area * vel**2
127     FL = cl * q_dyn
128     FD = cd * q_dyn
129
130     sa, ca = np.sin(alpha), np.cos(alpha)
131
132     Fx_aero = -FD * ca + FL * sa
133     Fz_aero = -FD * sa + FL * ca
134     Fy_aero = 0
135
136     F_body = np.array([Fx_aero, Fy_aero, Fz_aero])
137
138     Mx = (CR_r * wx * diameter / (2*vel)) * q_dyn * diameter
139     My = cm * q_dyn * diameter
140     Mz = CN_r * wz * q_dyn * diameter
141     M_body = np.array([Mx, My, Mz])
142
143     # Newton-Euler
144     F_aero_earth = R_IB.T @ F_body
145     F_gravity = np.array([0, 0, -m*g])
146     accel_earth = (F_aero_earth + F_gravity) / m
147
148     I_mat = np.diag([Ix, Iy, Iz])
149     omega_vec = np.array([wx, wy, wz])
150     term2 = np.cross(omega_vec, I_mat @ omega_vec)
151     dw_dt = np.linalg.inv(I_mat) @ (M_body - term2)
152
153     if np.abs(ct) < 0.001: ct = 0.001
154
155     dphi = wx + (wy * sp) * tt
156     dtheta = wy * cp
157     dpsi = (wy * sp) / ct
158
159     return [vx, vy, vz,
160             accel_earth[0], accel_earth[1], accel_earth[2],
161             dphi, dtheta, dpsi,
162             dw_dt[0], dw_dt[1], dw_dt[2]]
163
164     def hit_ground(t, state): return state[2]
165     hit_ground.terminal = True
166     hit_ground.direction = -1
167
168     # OPTIMIZED TOLERANCES
169     sol = solve_ivp(equations, (0, 15), initial_state, events=hit_ground, rtol=1e-3,
170                      atol=1e-6)
171     return sol
172 if __name__ == "__main__":

```

```
173 parser = argparse.ArgumentParser(description='3D Frisbee Flight Simulator')
174 parser.add_argument('--velocity', '-v', type=float, default=DEFAULT_V0)
175 parser.add_argument('--spin', '-s', type=float, default=DEFAULT_SPIN_RPM)
176
177 args = parser.parse_args()
178
179 sol = simulate_3d_throw(args.velocity, args.spin, args.height,
180                         args.launch_angle, args.release_angle,
181                         args.tilt_angle, args.aoa,
182                         AIR_TEMP_C, AIR_PRESSURE_PA)
183
184 x, y, z = sol.y[0], sol.y[1], sol.y[2]
185
186 print(f"Dist: {x[-1]:.2f}m, Drift: {y[-1]:.2f}m")
```